

Supplementary materials for: High-level cognition during
story listening is reflected in high-order dynamic
correlations in neural activity patterns

Lucy L. W. Owen¹, Thomas H. Chang^{1,2}, and Jeremy R. Manning^{1,†}

¹Department of Psychological and Brain Sciences,
Dartmouth College, Hanover, NH

²Amazon.com, Seattle, WA

[†]Address correspondence to jeremy.r.manning@dartmouth.edu

November 13, 2020

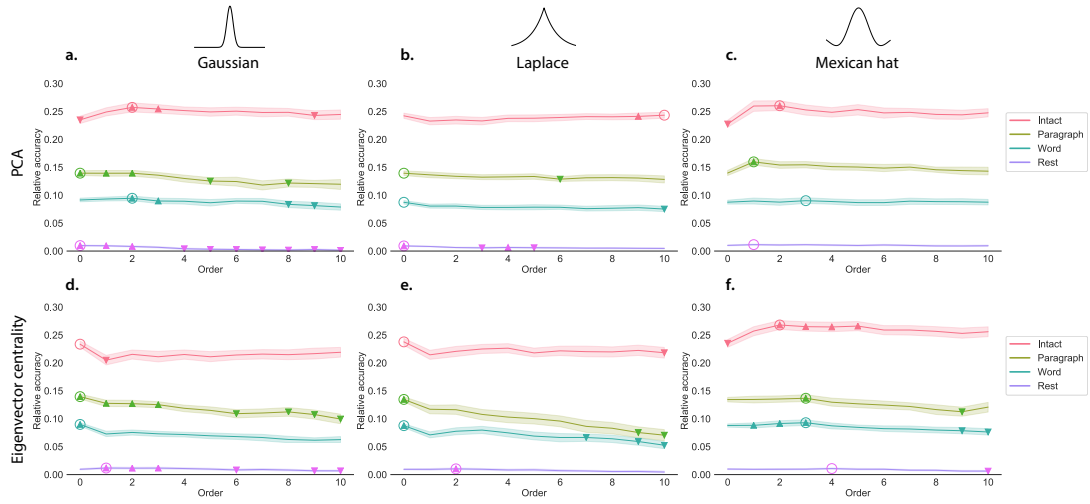


Figure S1: Across-participant timepoint decoding accuracy varies with correlation order and cognitive engagement across kernels. a.-c. Timepoint decoding accuracy as a function of order: PCA. *Order* (x -axis) refers to the maximum order of dynamic correlations that were available to the classifiers (see *Feature weighting and testing*). The reported across-participant decoding accuracies for **a. Gaussian**, **b. Laplace**, and **c. Mexican hat** kernels are averaged over all widths (see *Identifying robust decoding results*). The y -values are displayed relative to chance accuracy (intact: $\frac{1}{300}$; paragraph: $\frac{1}{272}$; word: $\frac{1}{300}$; rest: $\frac{1}{400}$). The error ribbons denote 95% confidence intervals across cross-validation folds (i.e., random assignments of participants to the training and test sets). The colors denote the experimental condition. Arrows denote sets of features that yielded reliably higher (upwards facing) or lower (downward facing) decoding accuracy than the mean of all other features (via a two-tailed test, thresholded at $p < 0.05$). The circled values represent the maximum decoding accuracy within each experimental condition. Panels a.-c. used PCA to project each high-dimensional pattern of dynamic correlations onto a lower-dimensional space. **d.-f. Timepoint decoding accuracy as a function of order: eigenvector centrality.** This panel is in the same format as Panel a.-c., but here eigenvector centrality has been used to project the high-dimensional patterns of dynamic correlations onto a lower-dimensional space.

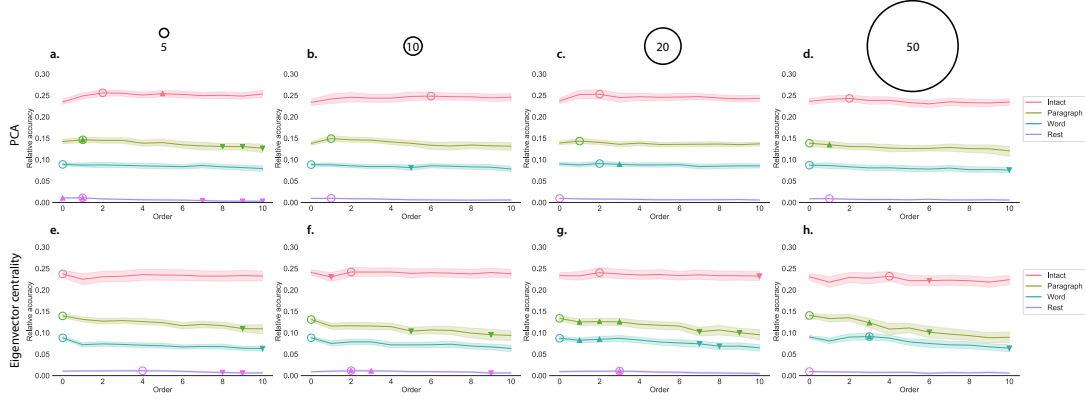


Figure S2: Across-participant timepoint decoding accuracy varies with correlation order and cognitive engagement across widths. a.-d. Timepoint decoding accuracy as a function of order: PCA. Order (x -axis) refers to the maximum order of dynamic correlations that were available to the classifiers (see *Feature weighting and testing*). The reported across-participant decoding accuracies for a. 5, b. 10, c. 20, and d. 50 are averaged over all kernel shapes (see *Identifying robust decoding results*). The y -values are displayed relative to chance accuracy (intact: $\frac{1}{300}$; paragraph: $\frac{1}{272}$; word: $\frac{1}{300}$; rest: $\frac{1}{400}$). The error ribbons denote 95% confidence intervals across cross-validation folds (i.e., random assignments of participants to the training and test sets). The colors denote the experimental condition. Arrows denote sets of features that yielded reliably higher (upwards facing) or lower (downward facing) decoding accuracy than the mean of all other features (via a two-tailed test, thresholded at $p < 0.05$). The circled values represent the maximum decoding accuracy within each experimental condition. Panels a.-d. used PCA to project each high-dimensional pattern of dynamic correlations onto a lower-dimensional space. e.-h. Timepoint decoding accuracy as a function of order: eigenvector centrality. This panel is in the same format as Panel a.-d., but here eigenvector centrality has been used to project the high-dimensional patterns of dynamic correlations onto a lower-dimensional space.



Figure S3: Top terms associated with the endpoints of the strongest correlations for the *intact* experimental condition. Each color corresponds to one order of inter-subject functional correlations. The inflated brain plots display the locations of the endpoints of the 10 strongest (absolute value) correlations at each order, projected onto the cortical surface (Combrisson et al., 2019). The lists of terms display the top 10 Neurosynth terms (Rubin et al., 2017) decoded from the corresponding brain maps for each order. (Also see Fig. 7, top row, in the main text.)

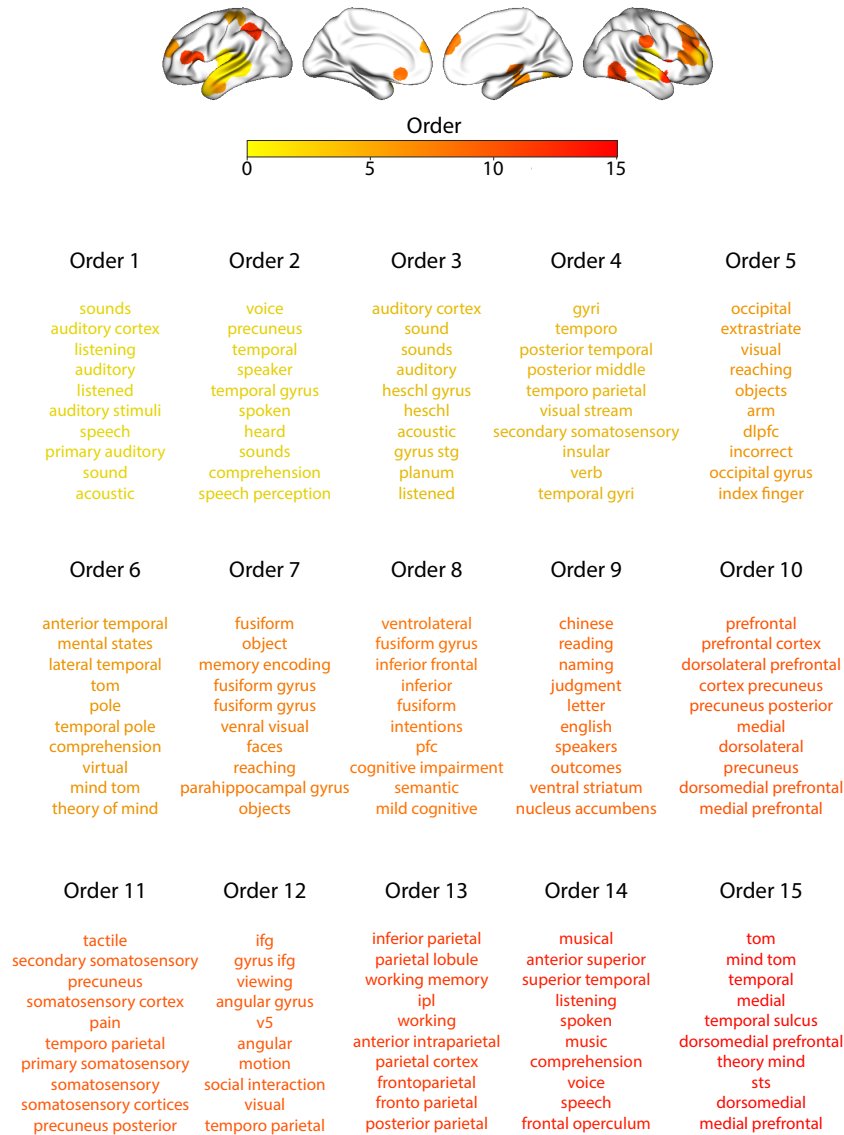


Figure S4: Top terms associated with the endpoints of the strongest correlations for the *paragraph* experimental condition. This figure is in the same format as Figure S3, but displays results for the paragraph-scrambled story listening condition. (Also see Fig. 7, second row, in the main text.)



Figure S5: Top terms associated with the endpoints of the strongest correlations for the *word* experimental condition. This figure is in the same format as Figure S3, but displays results for the word-scrambled story listening condition. (Also see Fig. 7, third row, in the main text.)



Figure S6: Top terms associated with the endpoints of the strongest correlations for the *rest* experimental condition. This figure is in the same format as Figure S3, but displays results for the resting state condition. (Also see Fig. 7, bottom row, in the main text.)

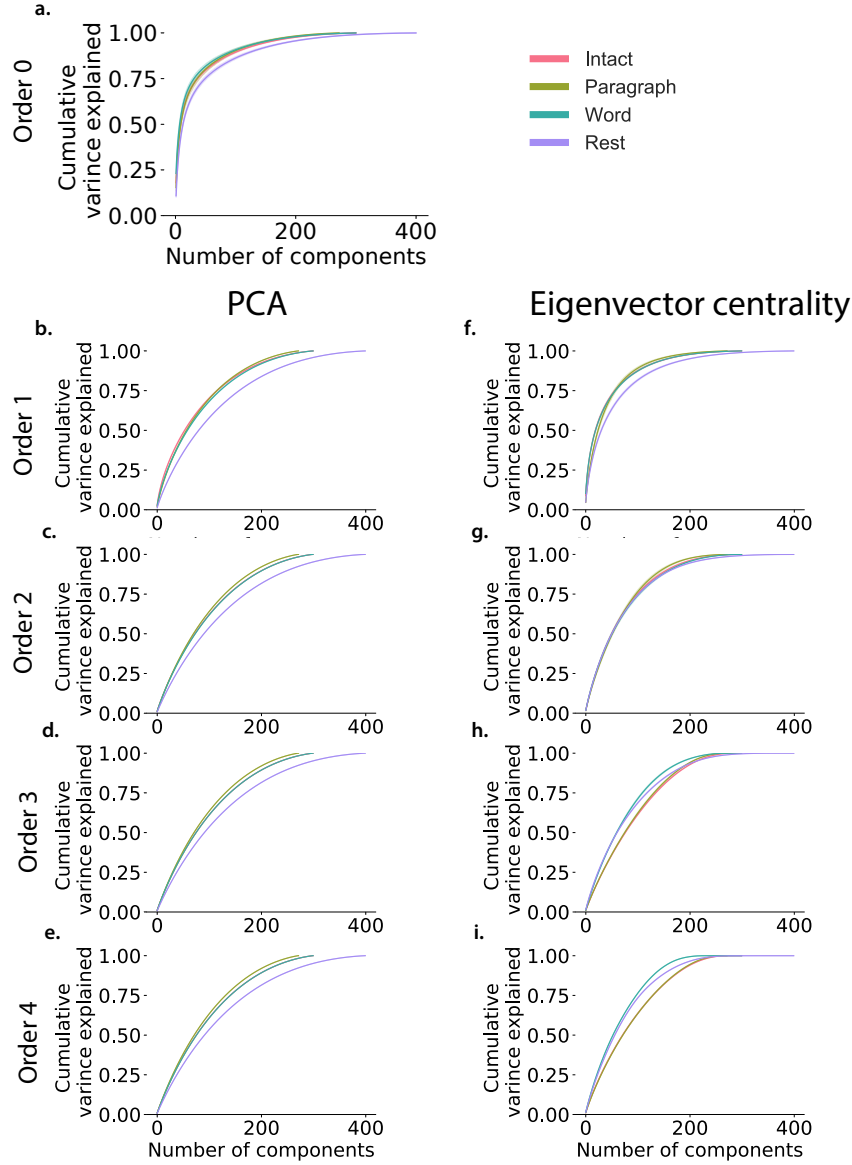


Figure S7: Cumulative percent variance explained as a function of the number of principle components for correlation orders and reduction types. *Order* refers to the order of the dynamic correlations calculated. Principle components analysis was performed, and reduced independently for each subject. Maximum number of components varies with the total time for each condition (intact: 300; paragraph: 272; word: 300; rest: 400). **a. Cumulative percent variance as a function of number of components for Order 0.** PCA was performed on the raw activity patterns (Order 0). **b.-e. Cumulative percent variance as a function of number of components for Orders 1-4: PCA** Dynamic correlation were calculated for orders 1-4 using PCA to project each high-dimensional pattern of dynamic correlations onto a lower-dimensional space. **f.-i. Cumulative percent variance as a function of number of components for Orders 1-4: eigenvector centrality.** These panels are in the same format as Panel b.-e., but here eigenvector centrality has been used to project the high-dimensional patterns of dynamic correlations onto a lower-dimensional space.

Supplementary references

- Combrisson, E., Vallat, R., O'Reilly, C., Jas, M., Pascarella, A., l Saive, A., Thiery, T., Meunier, D., Altukhov, D., Lajnef, T., Ruby, P., Guillot, A., and Jerbi, K. (2019). Visbrain: a multi-purpose GPU-accelerated open-source suite for multimodal brain data visualization. *Frontiers in Neuroinformatics*, 13(14):1–14.
- Rubin, T. N., Kyoejo, O., Gorgolewski, K. J., Jones, M. N., Poldrack, R. A., and Yarkoni, T. (2017). Decoding brain activity using a large-scale probabilistic functional-anatomical atlas of human cognition. *PLoS Computational Biology*, 13(10):e1005649.